CHAPTER 3

METHODS OF FATIGUE ANALYSIS AND A CASE STUDY

3.1 General

As per ASTM (ASTM 2000) fatigue can be defined as

"The process of progressive localized permanent structural change occurring in a material subjected to conditions that produce fluctuating stresses and strains at some point or points and that may culminate in cracks or complete fracture after a sufficient number of fluctuations."

The fatigue life is the number of cycles to failure at a specified stress level, while the fatigue strength (also referred to as the endurance limit) is the stress below which failure does not occur. There are various types of fluctuating stresses including fully reversed cycle (commonly used in laboratory testing), tension-tension fluctuation, compression-compression fluctuation, and random loading (Bridges are generally subjected to random loading). Typical loading cycles are illustrated in (Figure 3.1).

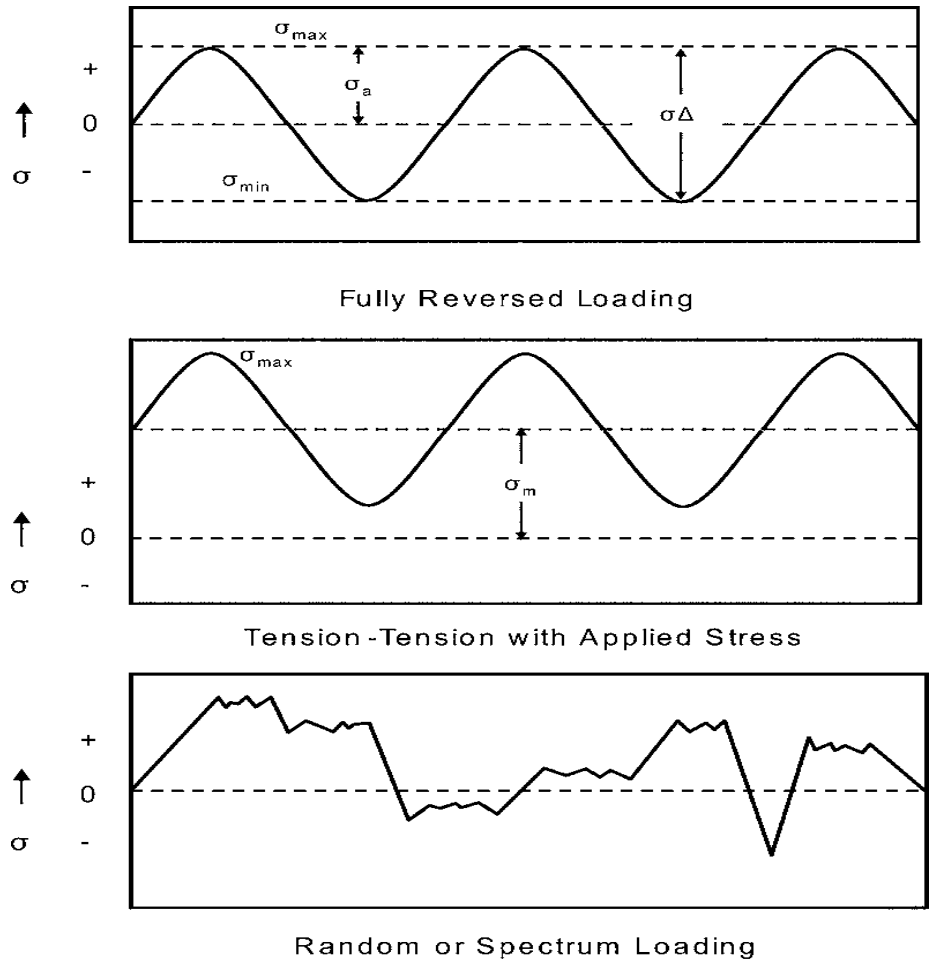

Figure 3.1: Typical loading cycles (Campbell 2008)
(Note: positive and negative sign denotes the tension and compression respectively.)

3.2 Indian railways bridges

Various types of bridges are employed in the Indian railway network, each designed to cater to specific requirements. Among them are solid web (plate) girder bridges, featuring standard spans of 9.15m, 12.2m, 18.3m, and 24.4m. Open web (truss) girder bridges, with standard spans of 30.5m, 45.7m, 61.0m, and 76.2m, are commonly utilized in railway structures across India, as illustrated in Figure 3.2. Under slung bridges adhere to a standard span length of 30.5m. Additionally, bow string girder bridges, predominantly employed in

road over bridges (ROB), contribute to the diverse array of bridge types in the Indian railway infrastructure.

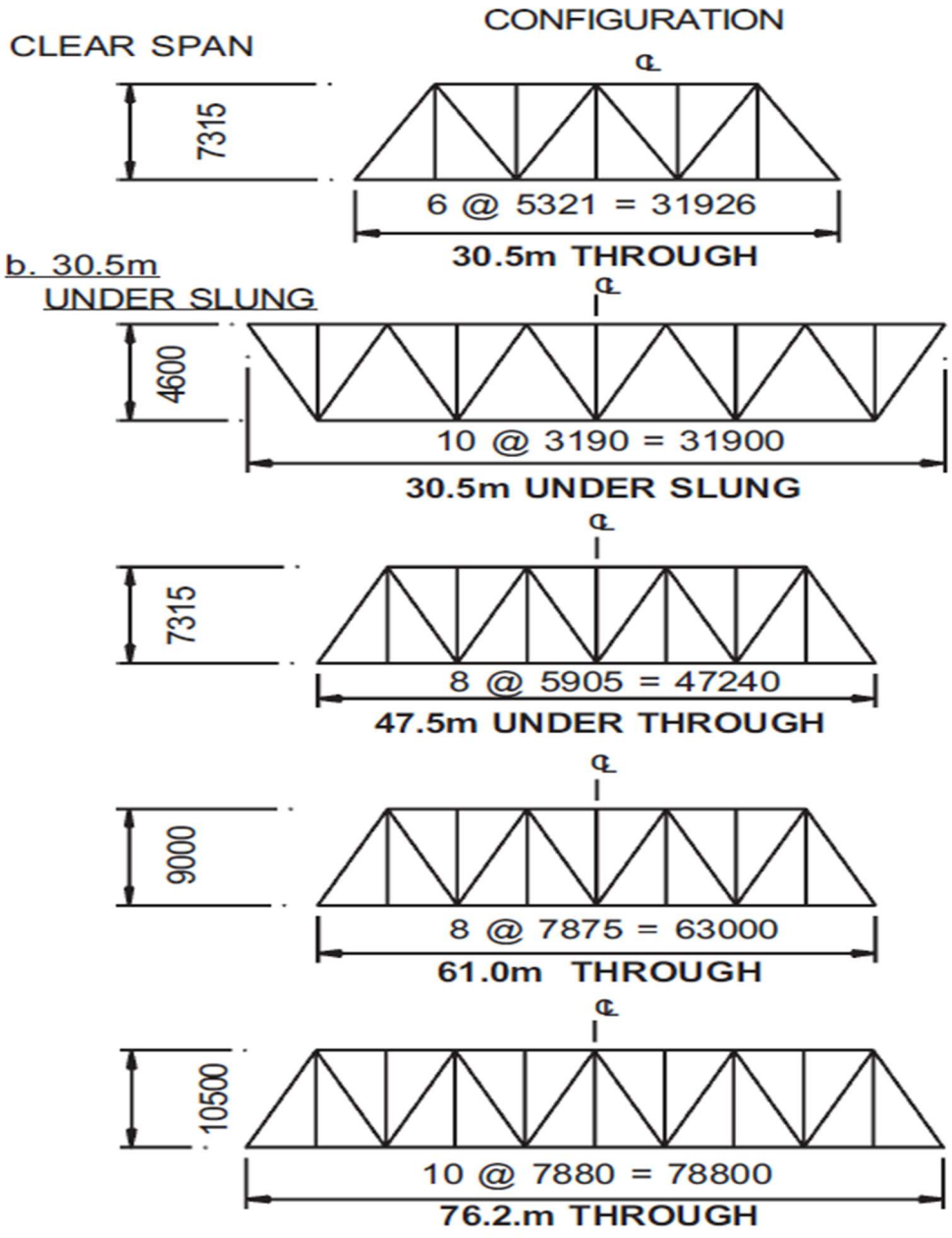

Figure 3.2: Standard spans of Indian railways truss bridges (IRICEN 2016)

As per Bridge Sub-Structures & Foundation Code (RDSO 2013), different types of railway bridges are defined as

1. Important bridges are those having a linear waterway of 300m or a total waterway of 1000m^2 or more.
2. Major bridges are those which have either a total waterway of 18m or more or which have a clear opening of 12m or more in any one span.
3. Bridges classified as minor bridges are those that do not fall under the important or major bridge categories.

3.3 Fatigue

3.3.1 Factors affecting life of structures

Factors influencing the service life of structures are corrosion-fatigue, deterioration damage, creep and shrinkage, and fatigue and fracture. Corrosion-fatigue results from cyclic stresses and a corrosive environment, accelerating metal failure. Deterioration, influenced by various factors, leads to structural damages such as efflorescence and rust stains. Creep, a time-dependent deformation at high temperatures and constant stress, affects long-term structural performance. Shrinkage and creep, related to hydrated cement paste, induce forces impacting structural members. Fatigue and fracture, cumulative damage processes, are significant considerations in structures subjected to cyclic loads. Fatigue, associated with variable loading, can lead to premature failure, with factors like loading sequence and material properties affecting fatigue strength.

The evaluation of these factors is crucial in determining the remaining service life of structures, particularly bridges.

The fatigue strength of a metal depends upon maximum stress, minimum stress, frequency of the loading cycles, nature of the load (fully reversal or tension-tension or random), and grade of metal.

3.3.2 Fatigue design criteria

Fatigue design criteria have moved from so-called infinite life to damage tolerance. Depending on the application, each of the successively evolved criteria has a place. The fatigue design criteria include the use of fatigue life methods such as the stress-life method, strain life method, and LEFM method.

3.3.2.1 Infinite-Life Design

This design relies on keeping stresses below the metal's fatigue strength, assuming flawless initial material. It follows the S-N curve, best for components stressed within the elastic range with a clear endurance limit, as seen in steels. Engine valve springs are generally designed by this method.

While simpler and practical for situations with limited inspection, it tends to yield heavier designs due to its conservative nature, despite being overshadowed by more modern methodologies.

3.3.2.2 Safe-Life Design

Safe-life design assumes an initially flawless part with a defined lifespan to develop a critical crack size. Similar to infinite-life methodology, it considers components without initial flaws. Developed for parts under higher loads causing plastic strains, it employs

strain-based assessment techniques, using log strain (ε) versus log number of cycles (N). Roller bearings are examples of this design.

3.3.2.3 Fail-Safe Design

Fail-Safe Design assumes timely detection and repair of fatigue cracks to prevent failure. Originating in the aircraft industry to overcome weight constraints, it features multiple load paths and crack stoppers. In case of a primary load path failure, an alternate path takes over, ensuring structural integrity. Rigorous certification criteria and crack detection capabilities are integral to this methodology. Engines are fail-safe only in multiengine aircrafts.

3.3.2.4 Damage-Tolerant Design

Damage-tolerant design, a refinement of fail-safe design, assumes structures may contain cracks. It employs fracture mechanics to calculate crack growth rates, allowing scheduled inspections for timely repairs or retirements before cracks reach critical dimensions. In pressure vessel design “leak before burst” is an expression of this methodology.

3.3.3 Methods of fatigue analysis

We can classify fatigue assessment methods into three categories: Stress life method, Strain life method, and LEFM based method.

3.3.3.1 Stress life method

Various terms which are common during stress life based fatigue assessment method can be defined as follows:

Nominal stress: The direct, shear, principal, or equivalent stress within the original material or in a weld near a potential crack site, computed according to elastic theory and excluding stress concentration effects.

Stress history: The documentation or calculation of stress fluctuations at a specific point in a structure during a loading event.

Stress range: The mathematical difference between the highest and lowest points of a specific stress cycle obtained from a stress history.

Stress range spectrum: A histogram illustrating the frequency of various stress ranges recorded or computed for a particular loading event.

Design spectrum: The cumulative representation of all stress-range spectra throughout the designated lifespan of a structure, relevant to fatigue assessment.

Equivalent constant amplitude stress range: The constant-amplitude stress range that, when evaluated through Miner's summation, would yield the same fatigue life as the design spectrum.

Design life: The predetermined timeframe during which a structure is expected to operate safely, with an acceptable likelihood that fatigue-induced failure will not occur.

Fatigue life: The anticipated duration until fatigue failure transpires, considering the application of the design spectrum.

As per Miner rule (Miner 1945)

$$D = \sum r_i = \sum \frac{n_i}{N_i} \tag{3.1}$$

Where n_i denotes the specified number of repetitions corresponding to the i^{th} stress range. N_i is the number of repetitions to failure for i^{th} stress range, and r_i is the cycle ratio corresponding to the i^{th} stress range. D is the damage value, the structure is safe until the damage value is less than one.

Basquin equation (Basquin 1910) can be written as

$$Log_{10} N = Log_{10} K - m\ Log_{10} \sigma_r$$

$$N\sigma_r{}^m = K \tag{3.2}$$

Where σ_r is range of stress or stress range in any one cycle, m is inverse slope of $log\sigma_r$/log N curve, N is number of repetitions to failure at the stress range σ_r. K, m are material empirical constants depending upon detail class. Detail class depends upon the type of connection used in the structure. For particular detail class K, m is a constant value.

Flow chart for stress life method is illustrated in Figure 3.3.

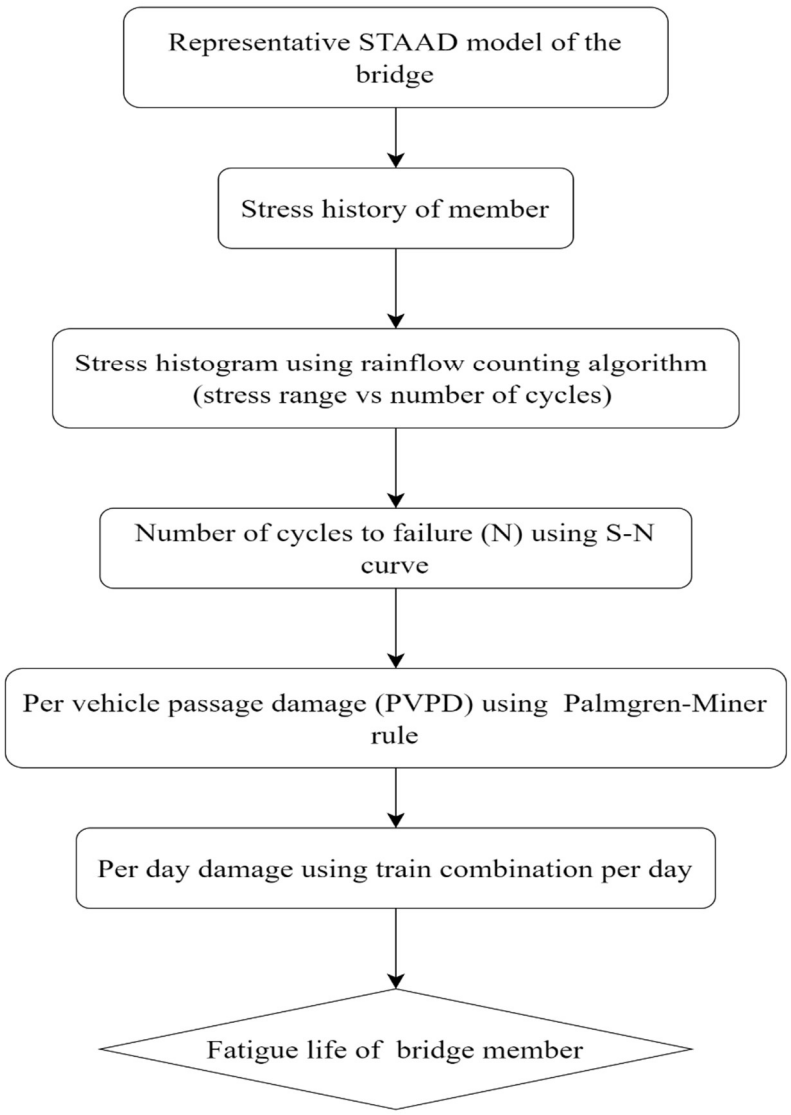

Figure 3.3: Flow chart for life of bridge using stress-life method

3.3.3.2 Strain life method

The strain-life approach was established in the 1960s and is relevant when strain incorporates a plastic component, suggesting a deviation from strictly elastic behaviour. This approach is especially useful in cases where fatigue lifetimes are short, such as the Low-Cycle Fatigue (LCF) regime. Low-cycle fatigue tests and the theoretical strain-life

technique have been used in some research to investigate the fatigue performance of steel bridges. Jesus et al. (2011), for example, published crack propagation fatigue data from five historic metallic riveted bridges in Portugal, connecting strain-life fatigue data using both deterministic and probabilistic models. However, research on fatigue life evaluation of steel bridges using the strain-life method has been limited, owing to the fact that the majority of fatigue problems in steel bridges are connected with the High-Cycle Fatigue (HCF) regime.

3.3.3.3 Linear Elastic Fracture Mechanics (LEFM) based approach

The mechanics of fatigue failure can be summarized as:

Small cracks may appear first in a fatigue failure; these cracks may be so small as to be undetectable. The crack typically appears when there is a localised concentration of stress, such as a welded junction, a keyway, a hole, or a discontinuity in the material or geometry. After a crack starts, it spreads because of the increased stress concentration effect. As a result, the component fails suddenly because the last region cannot support the load and the stressed area shrinks in size while the stress grows in magnitude. This leads to the fracture propagating more quickly. As a result, fatigue loading causes an unexpected and abrupt failure. Stages of fatigue failure mostly occurs in three stages (Figure 3.4), namely

I. Crack initiation (No crack propagation)
II. Stable crack growth (Paris law is applicable at this stage only)
III. Rapid crack growth (In this region, the slope of the curve starts increasing, reflecting the change in behaviour towards an unstable crack propagation)

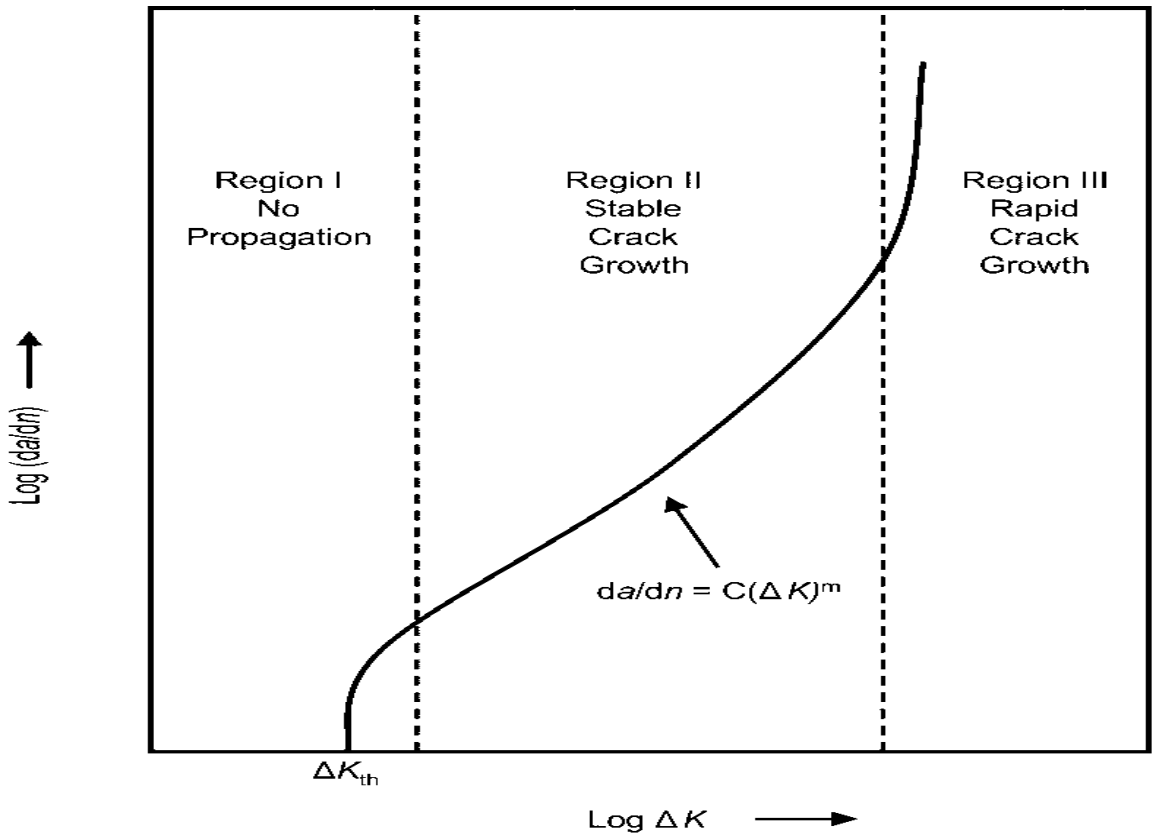

Figure 3.4: Crack propagation curve for fatigue loading (Campbell 2008)

There are many assumptions in the LEFM approach and unpredictable behaviour which shows its less adaptability. In LEFM approach, the equation given by Paris (1964) for fatigue crack propagation under cyclic loading is used to assess fatigue life. Equation given by Paris

$$\frac{da}{dN} = A \times (\Delta K)^n \tag{3.3}$$

$$\Delta K = Sr \times \alpha \times \sqrt{\pi a} \tag{3.4}$$

where a = crack length in ‘m’, N = number of repetitions, ΔK is the stress intensity factor measured in MPa$\sqrt{m}$, It depends upon material properties like size, shape, and crack orientation. A and n are constants depending upon material properties and environment. As crack growth rate data corresponding to fatigue is not available for a particular grade of steel (mild steel) used in the bridge, conservative values of A, n suggested by Barsom (Barsom 1971) are used. Sr denotes the stress range (in MPa) and α is the dimensionless parameter.

3.3.4 Standard provisions for fatigue assessment

In evaluating the remaining lifespan of an existing bridge through the stress-life method, the fundamental requirement for fatigue assessment involves the utilization of S-N curves. These curves depict the relationship between the Stress Range and the corresponding Fatigue Life 'N,' measured in terms of the number of stress cycles until failure. The establishment of these curves entails conducting fatigue tests in the laboratory using representative samples, resulting in diverse values of the number of cycles until failure for each stress range. The formulation of S-N curves is grounded in data derived from full-size specimens of diverse connection types, and their categorization is contingent upon the specific type of connection. It is imperative to select an appropriate S-N curve for the relevant connection type, as failure to do so may lead to varied assessments of fatigue life.

Standard S-N curves for different connection details are available with international codes like EN 1993-1-9, BS:5400 Part-10, IS: 800, and AREMA. The provisions outlined in these standards are summarized in the following paragraphs.

3.3.4.1 Eurocode EN 1993-1-9

The fatigue strength for nominal stress ranges is depicted through S-N curves, aligning with typical detail categories. Each detail category is identified by a numerical value representing the reference value $\Delta\sigma_C$ and $\Delta\tau_C$ for fatigue strength at $2x10^6$ N/mm^2.

Three different stress range levels characterise those strength curves:

- Constant amplitude fatigue limit ($\Delta\sigma_D$): The range of direct stresses below which no damage occurs, assuming a constant amplitude loading. In cases of variable amplitude loading, damage will be absent if all stress cycles have a range lower than this specific value.
- Cut-off limit ($\Delta\sigma_D$ or $\Delta\tau_L$): The value of direct or shear stress range below which cycles do not contribute to the accumulation of damage.
- Detail category ($\Delta\sigma_C$ or $\Delta\tau_C$): The reference strength for fatigue, corresponding to $N = 2 \times 10^6$.

(a) S-N curves and fatigue strength for normal stresses:

There are 14 S-N curves for direct stresses defined by EN 1993-1-9, which correspond to 14 distinct levels of fatigue strength. Each curve is identified and characterised by its reference value, $\Delta\sigma_C$. Standard S-N curves for normal and shear stresses are depicted in Figure 3.5 and Figure 3.6 respectively.

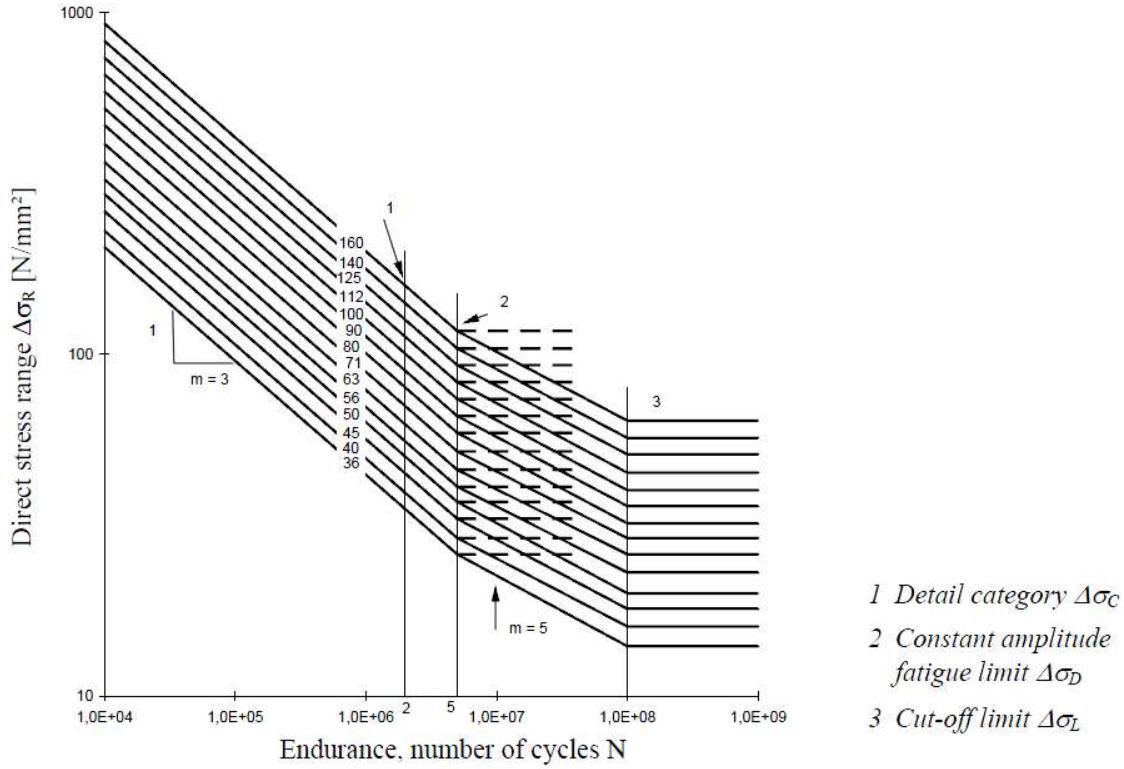

Figure 3.5: S-N curves for normal stress ranges (CEN 2005)

For constant amplitude stress ranges,

$$N_R = \begin{cases} \text{Infinite} ; \Delta\sigma_R \leq {\Delta\sigma_D}/{\gamma_{Mf}} \\ 5 \times 10^6 \times \left(\dfrac{{\Delta\sigma_D}/{\gamma_{Mf}}}{\Delta\sigma_R} \right)^3 ; \Delta\sigma_R \geq {\Delta\sigma_D}/{\gamma_{Mf}} \end{cases} \quad (3.5)$$

For nominal stress spectra with stress ranges above and below the constant amplitude fatigue limit,

$$N_R = \begin{cases} \text{Infinite};\ \Delta\sigma_R \le {\Delta\sigma_L}/{\gamma_{Mf}} \\ 5 \times 10^6 \times \left(\frac{{\Delta\sigma_D}/{\gamma_{Mf}}}{\Delta\sigma_R}\right)^5;\ {\Delta\sigma_L}/{\gamma_{Mf}} \le \Delta\sigma_R \le {\Delta\sigma_D}/{\gamma_{Mf}} \\ 5 \times 10^6 \times \left(\frac{{\Delta\sigma_D}/{\gamma_{Mf}}}{\Delta\sigma_R}\right)^3;\ \Delta\sigma_R \ge {\Delta\sigma_D}/{\gamma_{Mf}} \end{cases} \quad (3.6)$$

Fatigue limit

$$\Delta\sigma_L = \begin{cases} 0.737 \times \Delta\sigma_C;\ N \le 5 \times 10^6 \\ 0.549 \times \Delta\sigma_D;\ 5 \times 10^6 \le N \le 10^8 \end{cases} \quad (3.7)$$

(b) S-N curves and fatigue strength for shear stresses:

Shear stress ranges are represented by S-N curves that have a linear segment with a slope of 1:5 and a cut-off determined at 100×10^6 cycles. Similar to direct stress S-N curves, the fatigue strength at 2×10^6 cycles is used to identify the shear stress S-N curves. Only two shear stress S-N curves for two different detail categories are shown in the EN1993-1-9 (Figure 3.6).

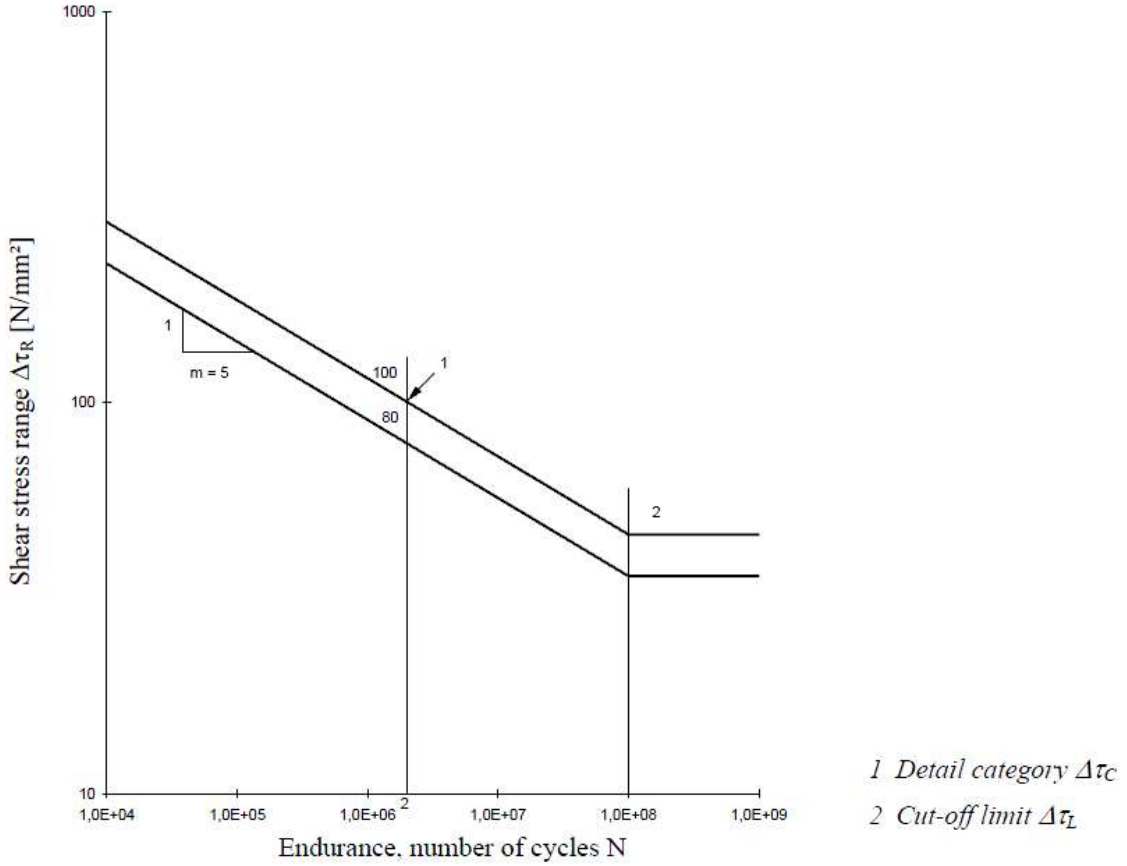

Figure 3.6: S-N curves for shear stress ranges (CEN 2005)

$$N_R = \begin{cases} \text{Infinite} ; \Delta\tau_R \leq {\Delta\tau_L}/{\gamma_{Mf}} \\ 2 \times 10^6 \times \left(\dfrac{{\Delta\tau_C}/{\gamma_{Mf}}}{\Delta\tau_R} \right)^3 ; \Delta\tau_R \geq {\Delta\tau_L}/{\gamma_{Mf}} \end{cases} \quad (3.8)$$

Where, N_R - number of cycles related to a constant stress range

$\Delta\sigma_R$, $\Delta\tau_R$ = normal and shear fatigue stress respectively, for N_R life cycle

Fatigue limit

$$\Delta\tau_L = 0.457 \times \Delta\tau_C \quad (3.9)$$

(c) Fatigue damage:

$$D_d = \sum_{i=1}^{n} \frac{n_{Ei}}{N_{Ri}} \tag{3.10}$$

D_d - damage

n_{Ei} – number of cycles corresponding to stress range $\gamma_{Ff}\Delta\sigma_i$ for band i in the factored spectrum

N_{Ri} - number of cycles to failure or endurance corresponding to stress range $\gamma_{Ff}\Delta\sigma_i$ for obtained from factored $\frac{\Delta\sigma_C}{\gamma_{Mf}} - N_R$ curve

γ_{Ff} – Partial factor for equivalent constant amplitude stress ranges $\Delta\sigma_E, \Delta\tau_E$

γ_{Mf} - partial factor for fatigue strength $\Delta\sigma_C, \Delta\tau_C$

3.3.4.2 British code BS 5400: Part10

In 2010, the Eurocodes superseded the British Standard BS5400 - Steel, concrete, and composite bridges in the United Kingdom for the design of new bridges. While the Structural Eurocodes now govern the design of new bridges, the assessment requirements for existing railway and highway infrastructure in the UK are still based on BS 5400.

Particularly noteworthy within BS 5400, in comparison to the Eurocodes, is Part 10 - Code of practice for fatigue (BSI, 1980). This section is significant for analysis as it considered additional factors related to the fatigue behavior of bridges. These factors include the categorization of more structural details, the explicit modeling of the probability of failure, and the direct incorporation of workmanship and inspection in detail categorization.

Similar to Eurocode 3, BS5400 outlines the strength of details with regard to fatigue using S-N curves. These curves establish the correlation between the number of cycles to failure, N, and the normal or tangential stress range, denoted by the symbol σ_R. Figure 3.0 illustrates the typical relationship between σ_R and N.

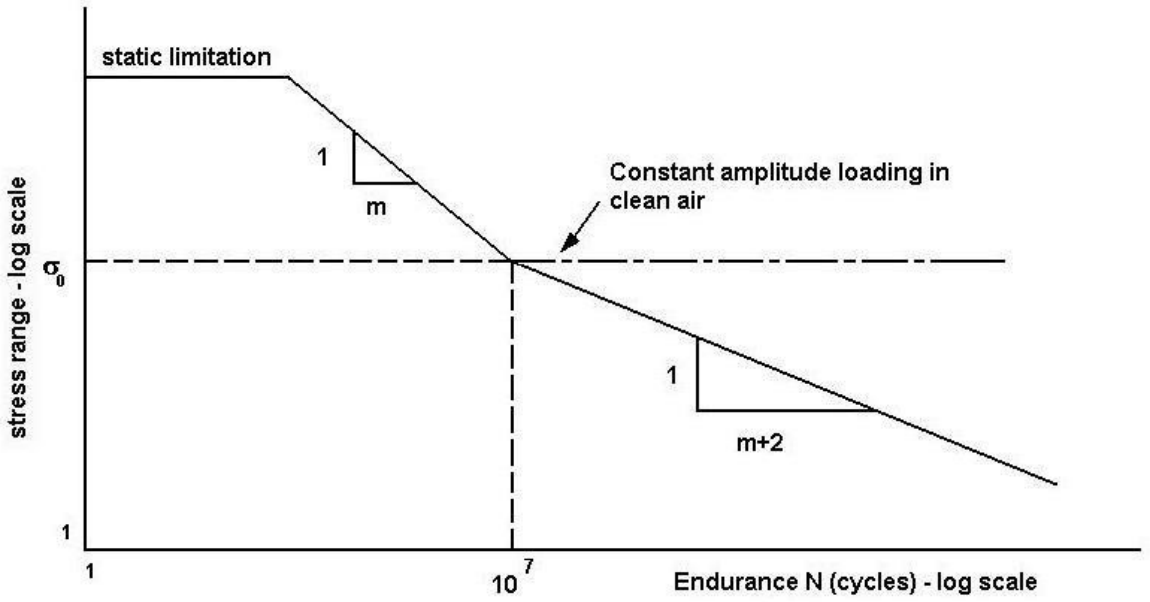

Figure 3.7: Typical $\sigma_R - N$ relationship (BSI 1980).

The concept introduced by BS 5400 is akin to Eurocode (CEN 2005), though with variations such as the use of σ_0 instead of $\Delta\sigma_D$. While Eurocode defines constant amplitude stress range for $N = 5 \times 10^7$, BS5400 defines it at $N = 1 \times 10^7$.

Fatigue loading impacts can be disregarded in non-welded details when the stress range solely falls within the compression zone. To determine the effective stress range for fatigue analysis, one should calculate it by adding 60% of the range from zero stress to the maximum compressive stress to the segment of the range from zero stress to the maximum tensile stress.

(a) S-N curves:

Unlike the Eurocodes, which distinguish S-N curves by three distinct stress ranges ($\Delta\sigma_C, \Delta\sigma_D, \Delta\sigma_L$), the S-N curves in BS5400 are characterized by a single stress range. It's essential to note that, in contrast to the single slope specified in Eurocode 3, the multiple S-N curves in BS5400 have various slopes. While Eurocodes describe 14 S-N curves for direct stresses, BS5400 defines only nine. However, BS5400 allows for the explicit consideration of different failure probabilities for each type of detail.

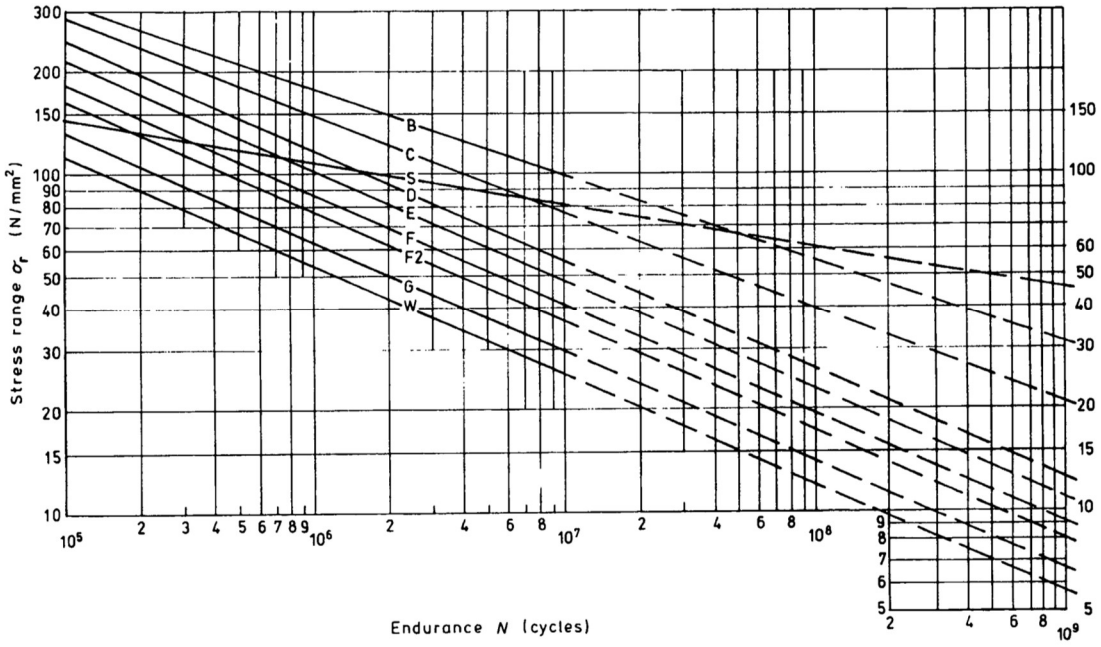

Figure 3.8: Design S-N curves (Probability of failure =2.3%) for different categories (BSI 1980)

Design σ_r − N relationship can be expressed in form of equation 3.11.

$$N \times \sigma_r^m = K_2 \quad (3.11)$$

Where N is number of repetitions or cycles to failure at stress range σ_r. Values of m, K_2 are provided in the BS 5400. Here K_2 correspond to a probability of failure of 2.3% within the design life.

Damage can be calculated by following equation (Equation 3.12)

$$\frac{n}{N} = \begin{cases} \frac{n}{10^7} \times \left(\frac{\sigma_r}{\sigma_0}\right)^m ; \ \sigma_r \geq \sigma_0 \\ \frac{n}{10^7} \times \left(\frac{\sigma_r}{\sigma_0}\right)^{m+2} ; \ \sigma_r \leq \sigma_0 \end{cases} \quad (3.12)$$

Considering probability of failure, equation 3.12 can be written as

$$N \times \sigma_r^m = K_0 \times \Delta^d \quad (3.13)$$

Where m is the inverse slope of mean line $\log \sigma_r - \log N$ curve

K_0 -constant term relating to the mean-line of the statistical analysis results

Δ - reciprocal of the anti-log of the standard deviation of log N

d - number of standard deviations below the mean-line. (This corresponds to a certain probability of failure as given below)

σ_r -Stress range in one cycle

σ_0 – constant amplitude non-propagating stress range (σ_r at $N=10^7$)

Table 3.1: Probability factors

Probability of failure (%)	50	31	16	2.3	0.14
d	0	0.5	1.0	2.0	3.0

(b) Specific categories:

Details are sorted based on the guidelines outlined in Table-17 of BS5400. The table comprises three distinct sections, each corresponding to fundamental categories for the classification of details: i) Non-welded features; ii) Welded details on the surface of the member; and iii) Welded details at the end connections of the member.

Additionally, BS5400 includes the classification of certain details not addressed in the Eurocodes, such as the categorization of riveted connections.

(c) Fatigue damage:

$$D = \sum_{i=1}^{n} \frac{n_i}{N_i} \quad (3.14)$$

D - damage

n_i – number of cycles corresponding to stress range σ_r for band i in the stress histogram

N_i - number of cycles to failure corresponding to stress range σ_r for obtained from S-N curve of required probability

3.3.4.3 Indian code IS 800

Guidelines provided by IRC 24 (IRC 2010) are exactly same as given in IS:800 (BIS 2007). Different particulars concerning members and connections are systematically grouped into specific fatigue classes for the purpose of fatigue-resistant design. Each fatigue class is associated with a designated design stress range corresponding to a specific number of cycles. S-N curve for normal and shear stress ranges is illustrated in Figure 3.9 and Figure 3.10 respectively.

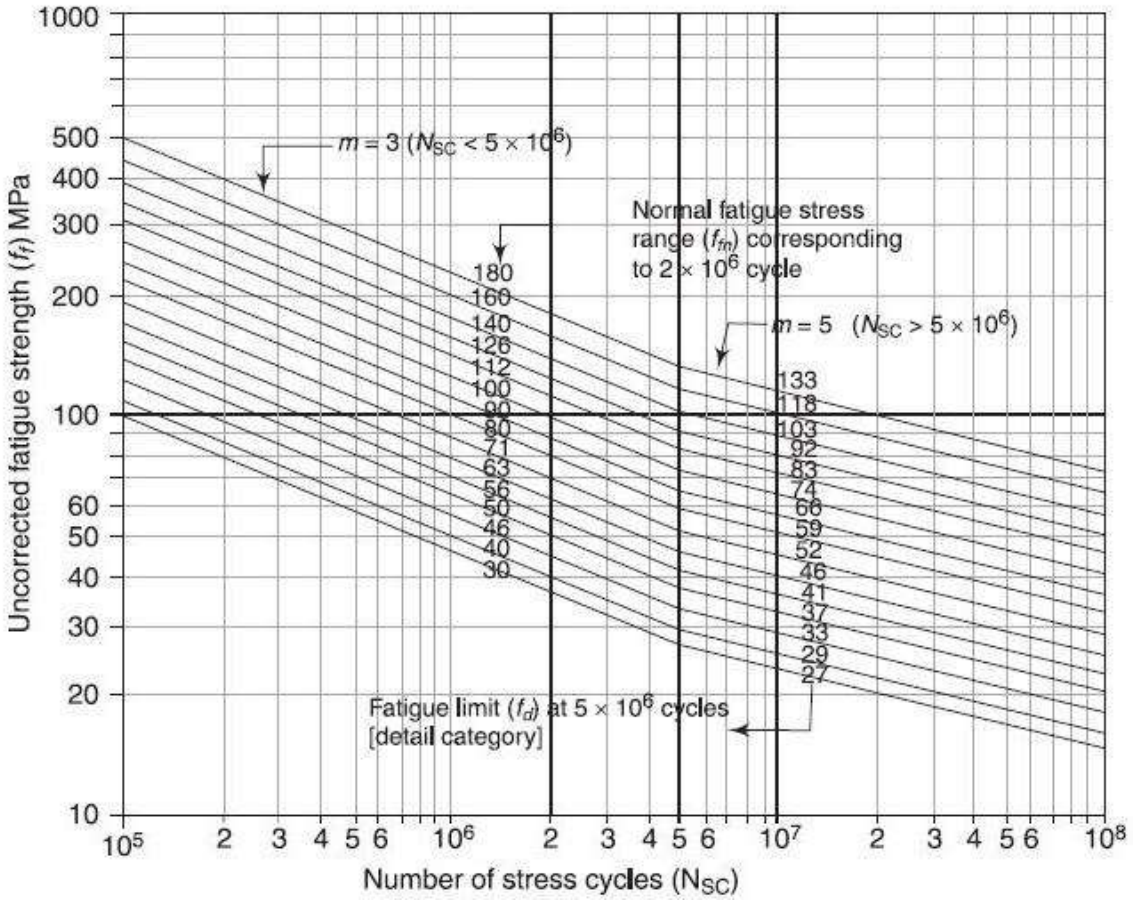

Figure 3.9: S-N curves for normal stress ranges (BIS 2007)

(a) Uncorrected fatigue strength:

The fatigue strength of the standard detail for the normal and shear fatigue stress range are

$$f_f = \begin{cases} f_{fn} \times \sqrt[3]{\frac{5 \times 10^6}{N_{SC}}}; & N_{SC} \leq 5 \times 10^6 \\ f_{fn} \times \sqrt[5]{\frac{5 \times 10^6}{N_{SC}}}; & 5 \times 10^6 \leq N_{SC} \leq 1 \times 10^8 \end{cases} \quad (3.15)$$

$$\tau_f = \tau_{fn} \sqrt[5]{\frac{5 \times 10^6}{N_{sc}}} \quad (3.16)$$

where, f_f, τ_f = Uncorrected normal and shear fatigue stress range respectively, for N_{SC} life cycle

f_{fn}, τ_{fn} = Normal and shear fatigue strength of the detail at 5×10^6 cycles, for the given detail category

N_{SC} = Number of stress cycles

The values derived from the standard S-N curve must be adjusted by a capacity reduction factor μ_r when transverse fillet or butt welding is used to connect plates thicker than 25 mm.

The degree of inspection capabilities and the effects of fatigue degradation have an impact on the partial safety factor for strength. It is necessary to apply a partial safety factor for fatigue strength.

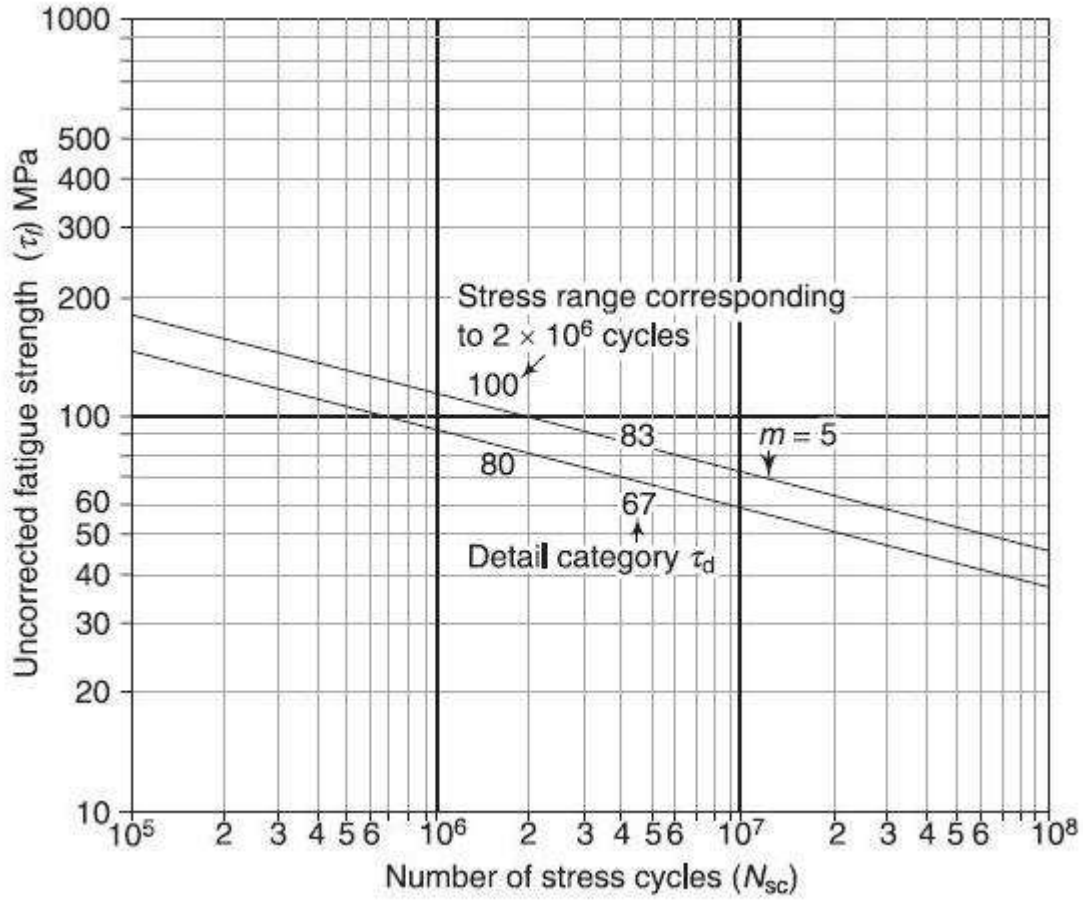

Figure 3.10: S-N curves for shear stress ranges (BIS 2007)

(b) Design fatigue strength:

For constants stress range,

$$f \leq f_{fd} = \frac{\mu_r \times f_f}{\gamma_{mft}} \tag{3.17}$$

$$\tau \leq \tau_{fd} = \frac{\mu_r \times \tau_f}{\gamma_{mft}} \tag{3.18}$$

μ_r- capacity reduction factor

γ_{mft} – partial safety factor against fatigue failure

f, τ – actual normal and shear stress ranges corresponding to detail category

(c) Fatigue stress limit:

No fatigue assessment is necessary for a member, detail or connection if any of the following conditions (Equation 3.19, 3.20, and 3.21) is valid.

Highest normal stress range

$$f_{t,max} \leq \frac{27 \times \mu_C}{\gamma_{mft}} \tag{3.19}$$

Highest shear stress range

$$f_{t,max} \leq \frac{67 \times \mu_C}{\gamma_{mft}} \tag{3.20}$$

Total number of actual stress cycles

$$N_{SC} \leq 5 \times 10^6 \left(\frac{27 \times \mu_C}{\gamma_{mft} \times f_{feq}} \right)^3 \tag{3.21}$$

Where μ_C- correction factor

f_{feq} denotes equivalent constant amplitude stress range (MPa).

3.3.4.4 American manual AREMA

Eight different S-N curves are provided in AREMA manual. In place of S-N curves following equation can also be used to find number of cycles corresponding to failure

$$N \times Sr^3 = A \tag{3.22}$$

Where N is number of repetitions or cycles to failure at stress range (Sr). Value of A corresponding to detail category is provided in the Table 15-1-9 of AREMA manual.

$$D_i = \frac{n_i}{N_i} = \frac{n_i}{A \times (Sr_i)^3} \tag{3.23}$$

Sr_i = Stress range of fluctuating stress corresponding to the number of cycles, n_i

N_i = Number of constant stress cycles which would cause fatigue damage equivalent to the fatigue damage caused by $\sum n_i$, of variable stress cycles

D-fatigue damage

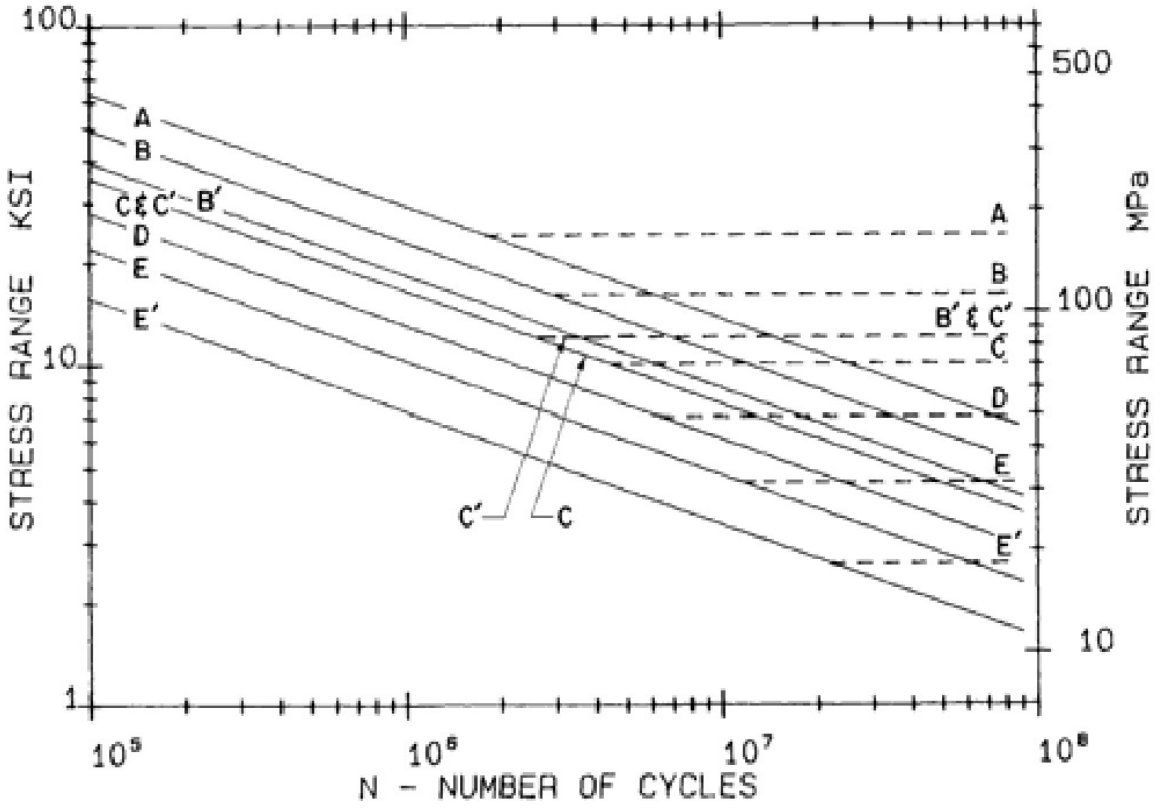

Figure 3.11: S-N curves for various detail categories (AREMA 2011)

3.4 Case study

Stress life method and LEFM method explained in section 3.3.3.1, 3.3.3.3 are used for fatigue based remaining life assessment of an existing steel railway bridge. The stress life method (S-N method) is suitable for the high cycle fatigue regime and steel railway bridges are subjected to a large number of variable stress cycles or repetitions during their lifespan. Number of repetitions to failure at a particular stress level is obtained using Basquin's equation (Basquin 1910) and cumulative damage is obtained as per Miner rule (Miner 1945). Report BS:91 (RDSO 2008) and British standard code (BSI 1980) have been used for the life assessment of the existing bridge. The rain flow counting method as per ASTM (ASTM 2017) is applied to convert varying amplitude stress response to fixed amplitude stress response for counting the load repetitions using MATLAB. Although there is no crack at present in the existing bridge but an initial crack length of 1.0mm is assumed for the remaining life assessment.

3.4.1 Bridge details and loading

(a) Bridge description:

The bridge over the Bhakra River is a single-track open web steel girder bridge between the Bareilly-Rampur section that belongs to the Moradabad division of India's Northern Railway shown in Figure 3.12.

Figure 3.12: Steel railway bridge in the Bareilly-Rampur section

Railway lines between Bareilly junction & Rampur junction, and the location of the bridge are shown in Figure 3.13. In order to get dimensional details of the bridge, site visit was carried out by the author. The existing railroad bridge has six spans, each measuring 30.5 meters. The bridge has steel superstructure, RCC bed block, Rocker, and roller-type bearing. Brick masonry piers were built over a well foundation. A satellite image of the truss bridge with labels is shown in Figure 3.14.

Figure 3.13: Railway lines between Bareilly and Rampur junctions and bridge location

(Source: indiarailinfo.com)

Figure 3.14: Satellite image of the bridge (Location: 28°31'22.0 "N, 79°15'04.4"E)

(Source: https://goo.gl/maps/3XAezZcNDCuMT33f6)

Line diagram of the steel railway bridge is shown in Figure 3.15.

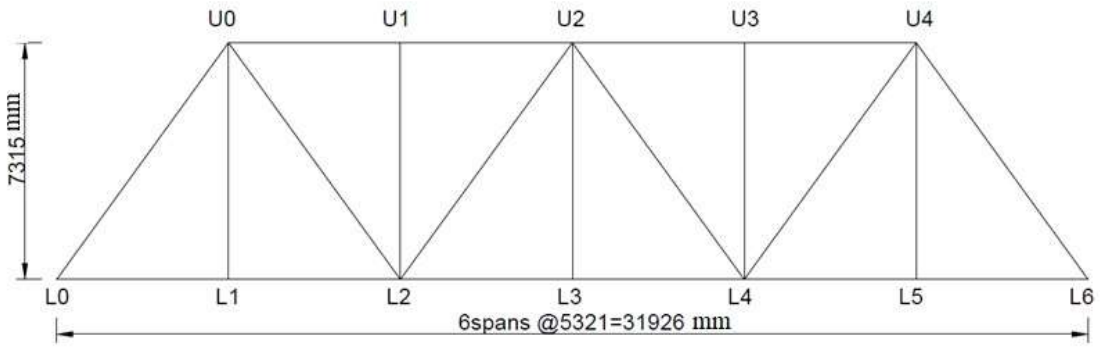

Figure 3.15: Configuration of the bridge members

(b) Traffic details:

Loading over the bridge is taken from 1950 onwards for the remaining life assessment. "25T loading -2008" loading is proposed over the bridge which has a higher axle load than current loading CC+8+2T and past loading like Modified Broad Gauge (MBG), Revised Broad Gauge (RBG), Broad Gauge Main Line (BGML) loading. Loading arrangement with axle load and axle spacing for passenger trains, empty freight trains, and loaded freight trains can be seen in Figure 3.16(RDSO 2014).

Due to the projected accelerated variation of GMT in the future, past traffic has also been taken into account as a rising variable instead of a constant one. Year-wise traffic density and combination of trains per day are presented in Table 3.2.

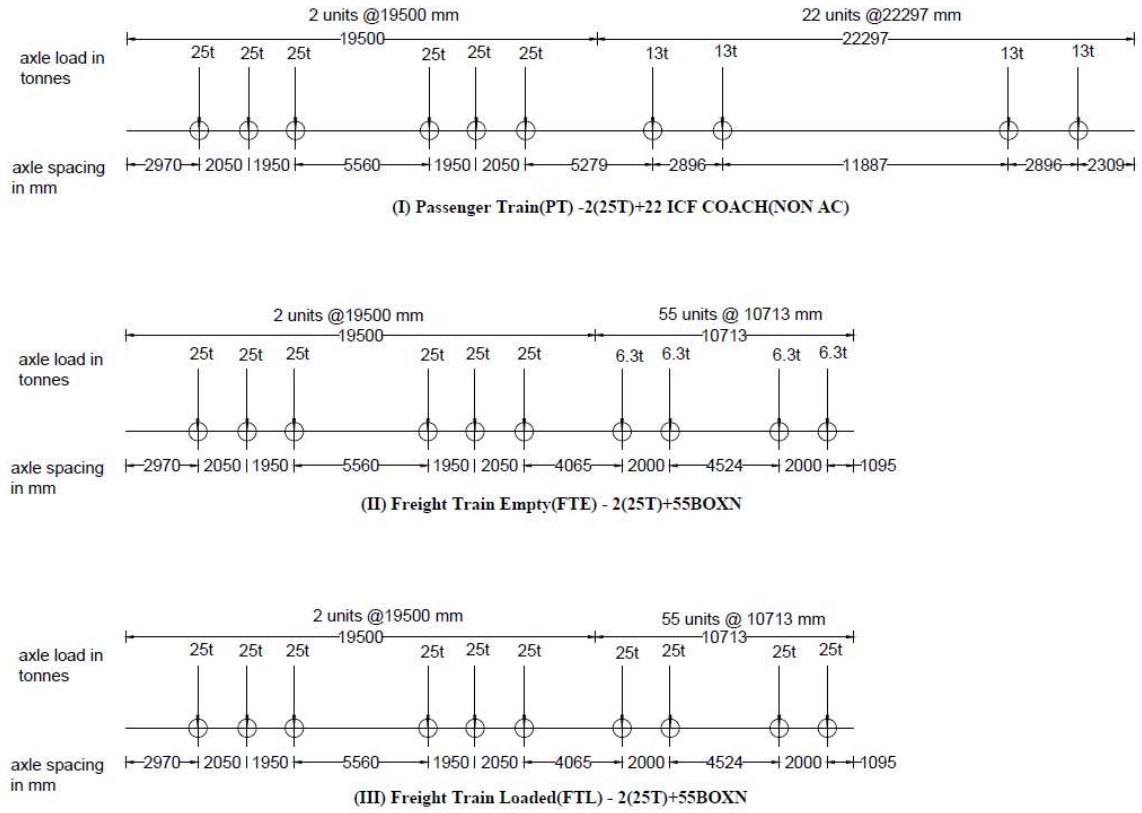

Figure 3.16: "25T-2008" loading as per bridge rules (data from RDSO 2014)

Table 3.2: Traffic combination details

Year	Traffic density (GMT)	Combination per day (PT+FTE+FTL)
1950-1975	20	13xPT+5xFTE+5xFTL
1975-2000	30	16xPT+8xFTE+8xFTL
2000-2025	40	25xPT+10xFTE+10xFTL
2025-2050	60	36xPT+15xFTE+15xFTL
2050-2075	80	50xPT+20xFTE+20xFTL

Where PT: 2+22 ICF NON-AC (GMT/train=0.51, length=524.25m),

FTE: 2(25T) + 55BOXN (GMT/train=0.61, length=624.15m),

FTL: 2(25T) + 55BOXN (GMT/train=2.12, length=624.15m).

GMT: Gross Million tonne, it is the total train load per year

The cumulative traffic density versus year graph has been shown in Figure 3.17.

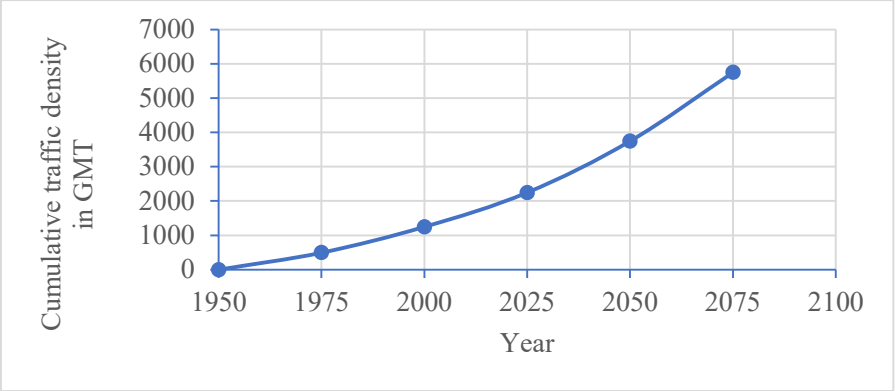

Figure 3.17: Cumulative traffic density over years

(c) Finite Element Modelling:

Experimental study of such a large bridge is a time taking and costly task. The bridge has been numerically simulated using the software STAAD CONNECT Edition. The bridge is modeled as a space frame structure in STAAD software using 2-noded beam elements. All the members of the bridge are built-up sections made-up of mild steel. Elastic properties of the material are Density = 7850 kg/m^3, modulus of elasticity =200 GPa, and Poisson ratio= 0.3. The single span of the bridge is modeled using beam elements. Although the provision of an Equivalent Uniformly Distributed Load (EUDL) in place of the actual axle load is mentioned in the bridge rule (RDSO 2014), axle loads are applied as point loads for more accurate analysis. The total number of beam elements and nodes in the STAAD model are 100 and 38 respectively. A total of 1900 load combinations (700 for FTE type train,700 for FTL type train, and 500 for PT type train) are generated for fatigue analysis of the bridge. STAAD model with an axle load of train and linear dimension of members is shown in Figure 3.18(a). STAAD model with node numbers and beam numbers can be seen in Figure 3.18(b) and Figure 3.18(c) respectively. A 3D structure diagram of the bridge modeled in STAAD is shown in Figure 3.19.

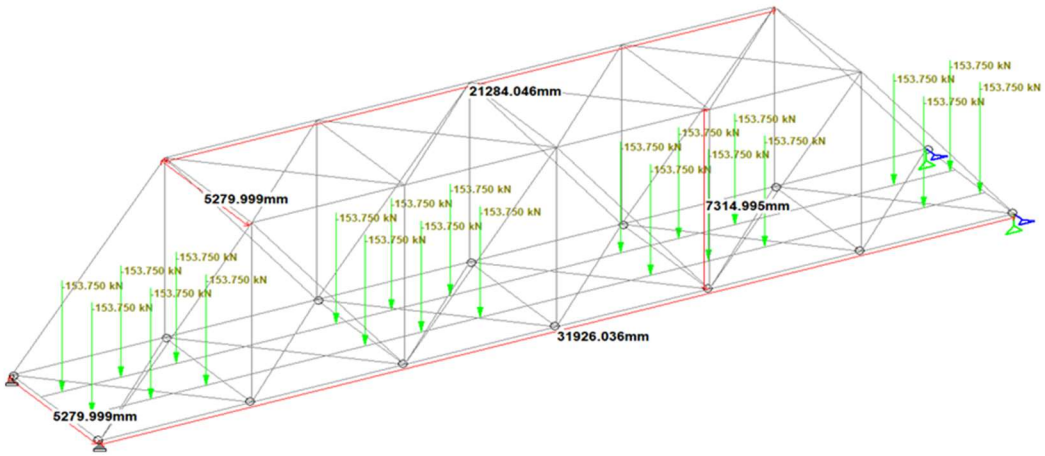

Figure 3.18(a): STAAD model of the bridge with a train load

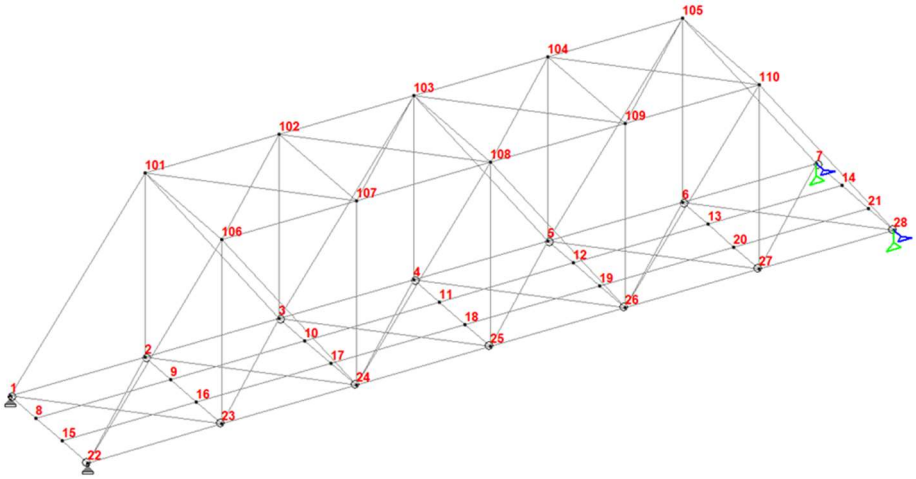

Figure 3.18(b): Bridge model with node number

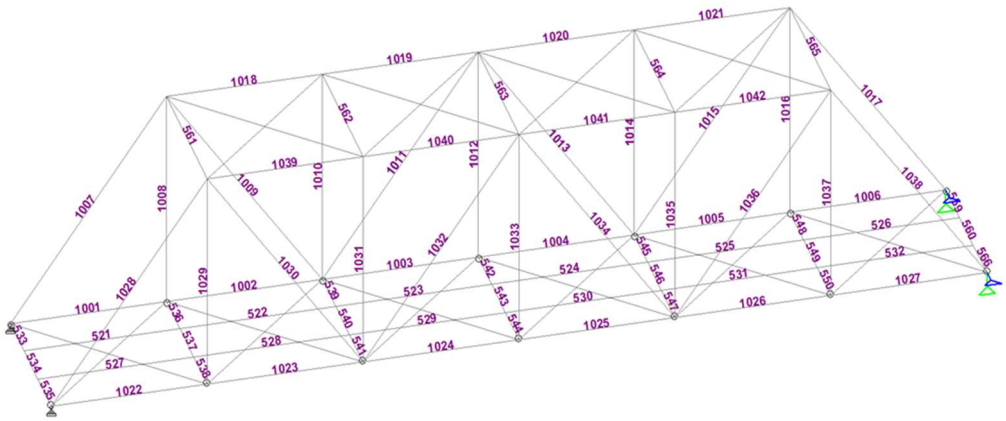

Figure 3.18(c): Bridge model with beam number

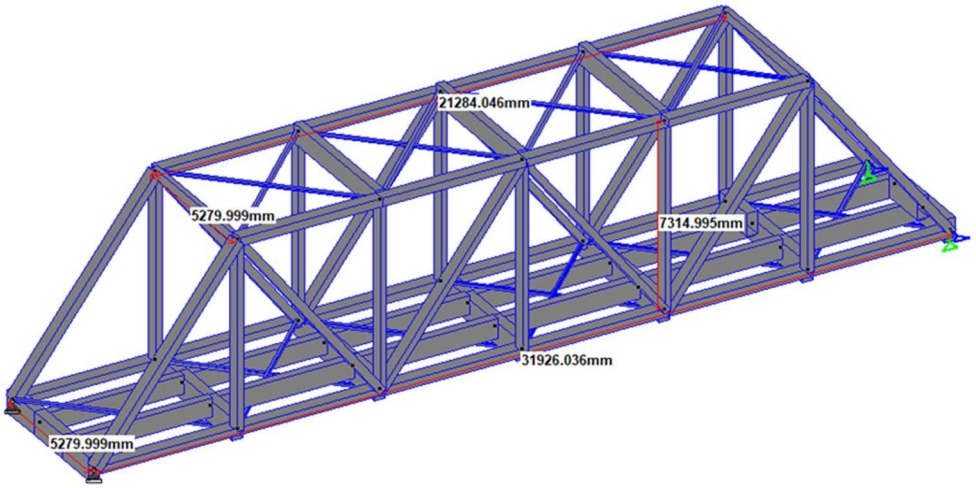

Figure 3.19: 3D model of the bridge using STAAD

Some important characteristics related to the model considering the existing bridge are

1. The web of the stringer and floor beam or cross beam is rigidly connected with the help of steel angle sections, so the rigid connection is provided between the stringer and cross beam in the STAAD model.
2. Rocker and roller bearings are provided as support, same nature of support conditions are applied in the model.
3. Built-up mild steel cross-sections in the model are provided using the user table function of STAAD software.
4. Proposed loading (25T loading -2008) is applied to the model to analyze the behavior of the bridge at increased axle load under three different speeds- up to 50kmph, equal to 80kmph, and equal to 125kmph.
5. Variation in stresses due to the live load is taken into account for fatigue analysis, but the stress due to the dead load of the bridge is not considered as it is not the fluctuating load.

6. Vehicle width, axle loads, and corresponding axle spacing have been defined under vehicle definition, and after providing the coordinate of the reference wheel with respect to the STAAD model's origin, the defined vehicle has been used under load generation function.

3.4.2 Remaining life assessment

The bridge's suitability and remaining life have been evaluated for both speed and GMT criteria at current as well as proposed levels to meet future requirements. The CC+8+2T loading (CC represents the carrying capacity) is currently traveling over the bridge at 40 GMT, and since there is no speed restriction across the bridge, freight trains typically go at 40 to 80 kmph while passenger trains typically travel at 50 to 100 kmph. As proposed loading over the bridge is "25T-2008" loading and the same has been taken in the remaining life assessment of the existing bridge. Static analysis has been performed using the bridge rule's coefficient of dynamic augment (CDA) (RDSO 2014). The impact load caused by trains passing over the bridge is calculated using the coefficient CDA at various speeds.

In this study two approaches as- stress life method and the fracture mechanics method have been used to assess the remaining fatigue life as discussed below

3.4.2.1 Remaining life using Stress life method

In this method, the stress history of identified critical members is obtained as a result of STAAD analysis. Using the rain flow counting method stress histogram is prepared, and the number of repetitions corresponding to failure are obtained by the S-N curve. The linear damage rule is applied to access the remaining life of the bridge.

A total of 1900 load combinations have been generated to represent the movement of actual trains over the bridge. Stress history (graph of load versus load generation) obtained by numerical analysis due to actual train load is converted into a stress histogram using the rain flow count method (ASTM 2017).

(a) Identified critical members:

Life of identified critical members, one member each from Bottom Chord(1003), Vertical member(1008), Diagonal member(1009), Stringer(523), Cross beam/Floor beam(543) has been calculated for a particular GMT, at a particular speed for stress band of 5 MPa and 10 MPa. Table 3.3 (which represents the total life of members for a constant traffic density of 30 GMT and a 50 kmph speed limit), shows that the cross-beam (543) at the mid-section is the most critical member of the bridge since the life of this member is the least among all selected members. So, life of cross beam (543) will be the governing member for the lifespan of the bridge.

Table 3.3: Total life of bridge members (years), for constant traffic density of 30 GMT and speed limit of 50kmph using the stress life method

	Member						
Stress band	L2L3 (1003)	L1U1 (1008)	L2U1 (1009)	L2U3 (1011)	L3U3 (1012)	Stringer (523) at end section	X-beam (543) at mid-section
5MPa	882.682	1250.84	651.56	805.93	801.20	440.22	265.05
10MPa	915.853	1050.55	655.29	894.60	707.02	349.74	234.66

Where 1003,1008,1009,1011,1012,523, 543 are member number given in Figure 3.7.

(b) Stress history:

The stress history diagram of critical member (Floor beam or cross beam-543) at speed of 80kmph is shown in Figure 3.20. It can be observed from Figure 3.20 that the stresses in PT are dropping to near zero, while this is not the case for FTE and FTL. From Figure 3.19, the center-to-center distance between the bridge's cross beams is 5.32m. From Figure 3.16, the center-to-center distance between the inner wheels of the passenger train coach and freight train wagon is 11.887m, and 4.524m, respectively. A load step of approximately 1m is taken during the moving load analysis in STAAD.

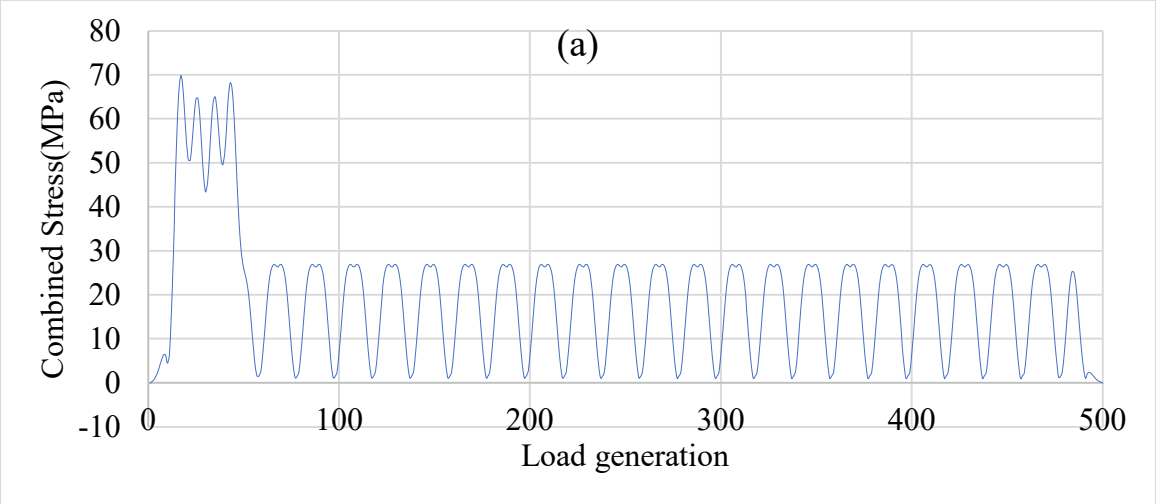

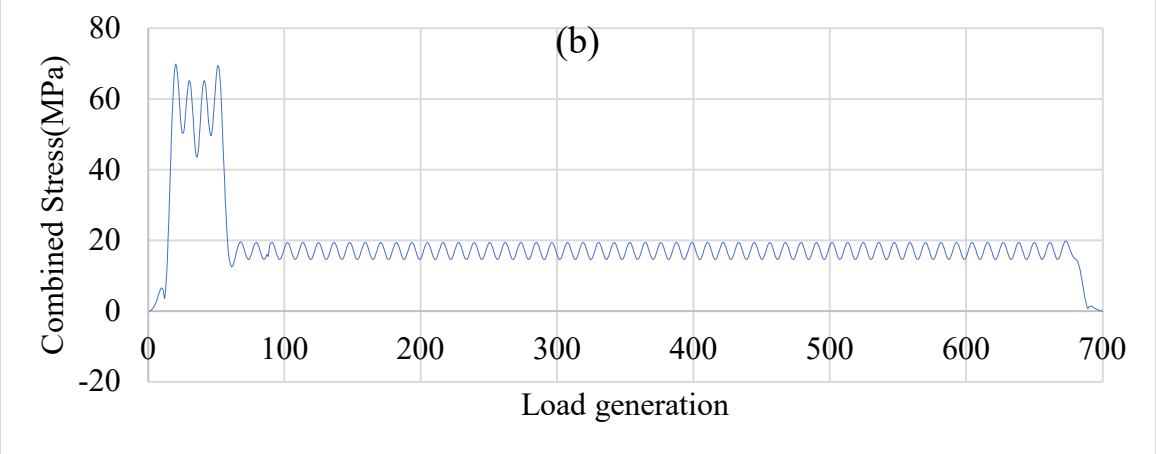

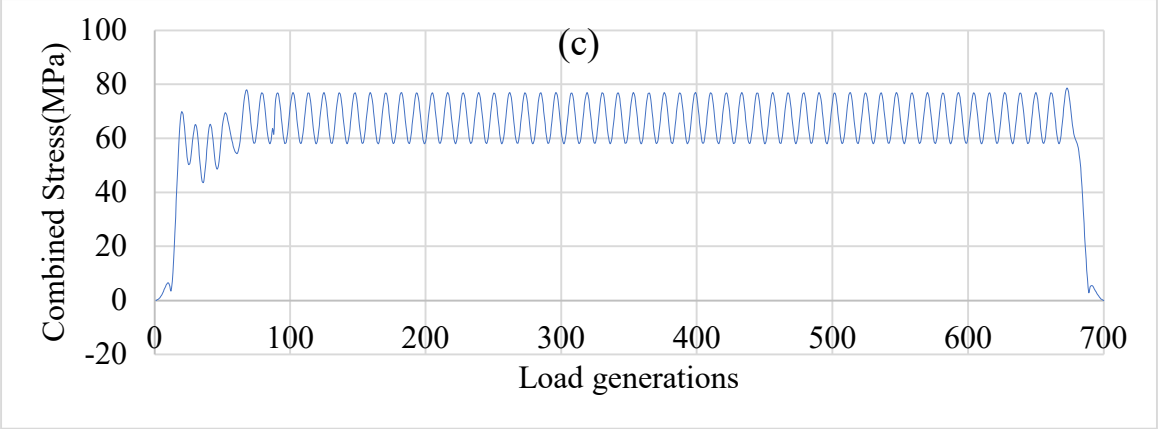

Figure 3.20: Stress history of a critical member (Floor beam or cross beam-543) at speed of 80kmph **(a)** for train PT **(b)** for train FTE **(c)** for train FTL

So the circumstance arises when the inner wheels of a passenger train coach are positioned exactly above adjacent cross beams of the bridge's considered cross beam (543). Since most of the load is taken by adjacent cross beams at that load step, the considered beam's stresses are almost zero. However, this is not the case for loaded or empty freight trains. Spacing between the inner wheels of freight train wagon is 4.524m, less than the center-to-center distance between cross beams, so adjacent cross beams do not take the whole load in any load step. Due to this, the considered cross beam (543) is constantly subjected to some load for both empty and loaded freight trains.

(c) Stress histogram:

Representative GMT which is varying at each 25 years interval is taken for the remaining life assessment of the steel truss bridge. The critical member for the bridge is the floor beam/cross beam "cross beam-543 at midsection". Stress histogram for a passenger train, empty freight train, and loaded freight train for "25T-2008" loading at speeds up to 50 kmph, equal to 80 kmph, and equal to125kmph with stress bands of 10 MPa and 5 MPa can be seen in Figure 3.21 and Figure 3.22 respectively.

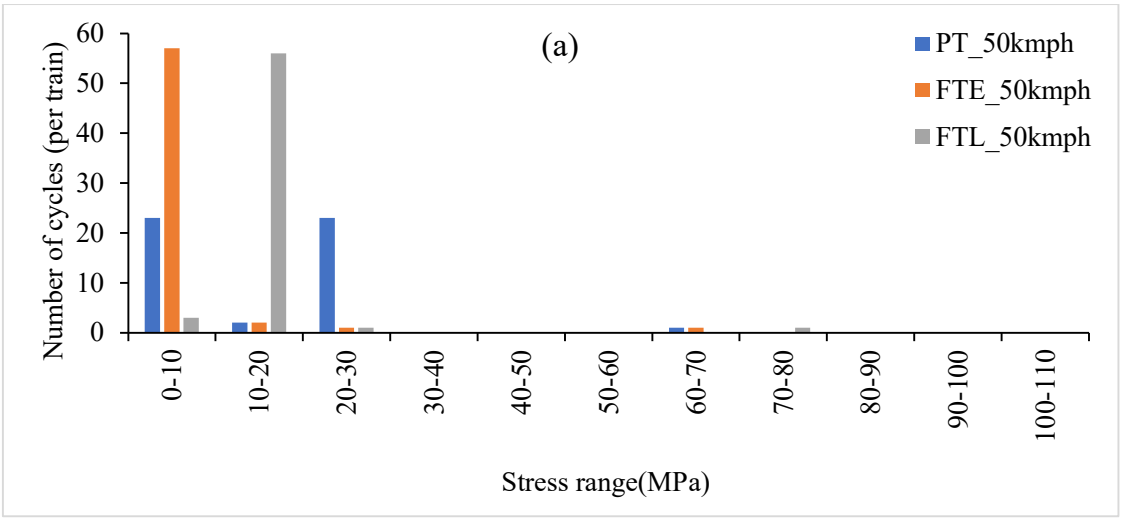

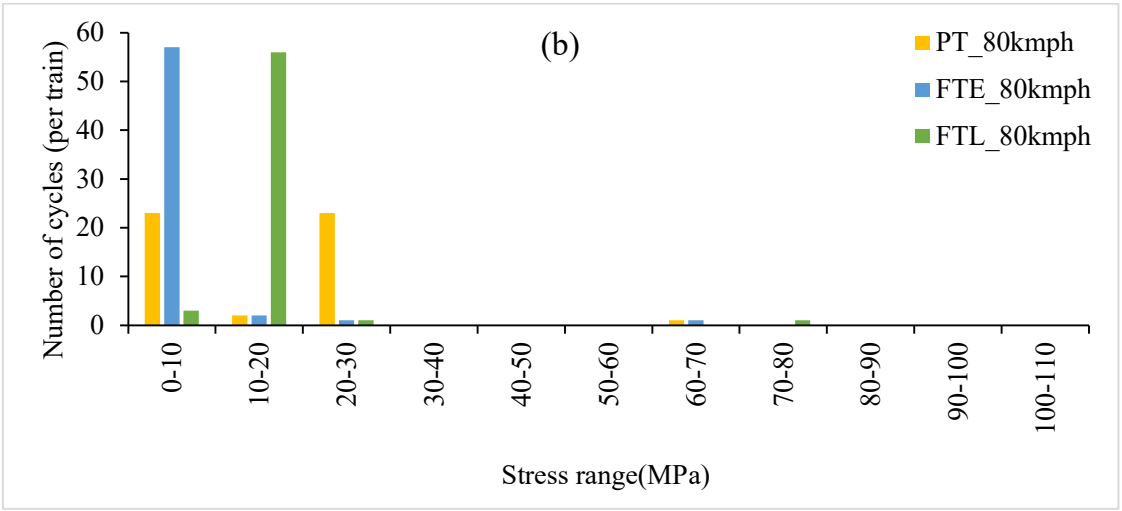

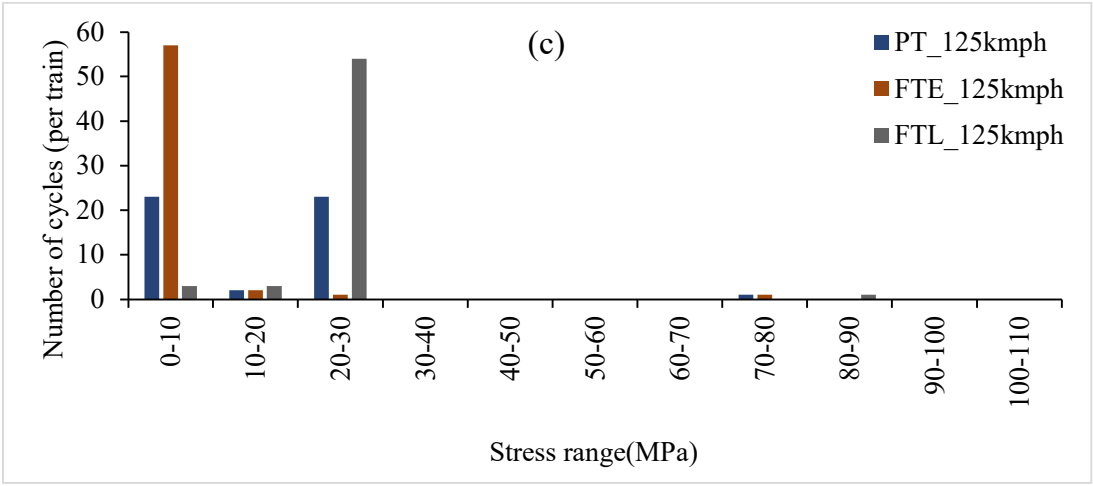

Figure 3.21: Stress histogram for member (cross beam-543 at mid) at stress band=10MPa **(a)** PT, FTE & FTL at speed up to 50kmph **(b)** PT, FTE & FTL at speed equal to 80kmph **(c)** PT, FTE & FTL at speed equal to 125kmph

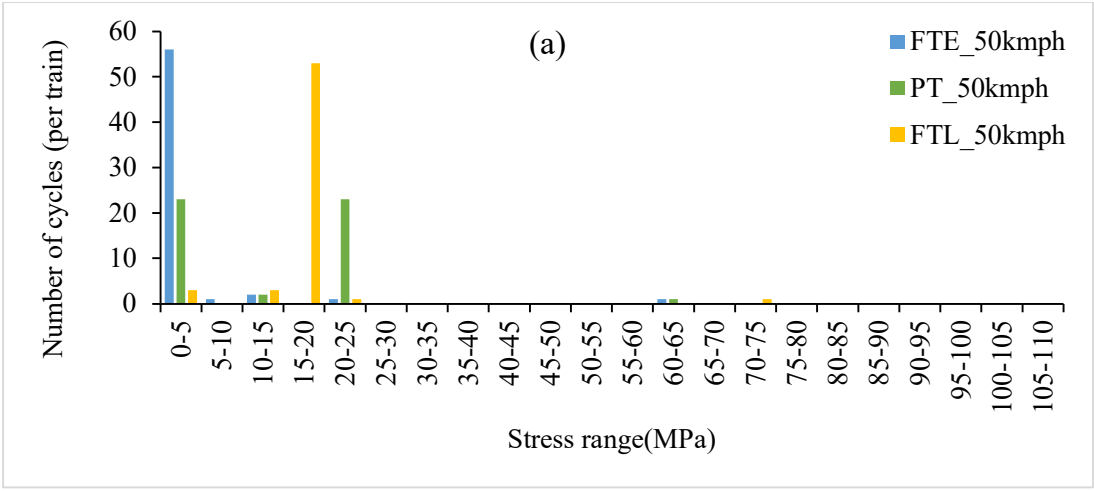

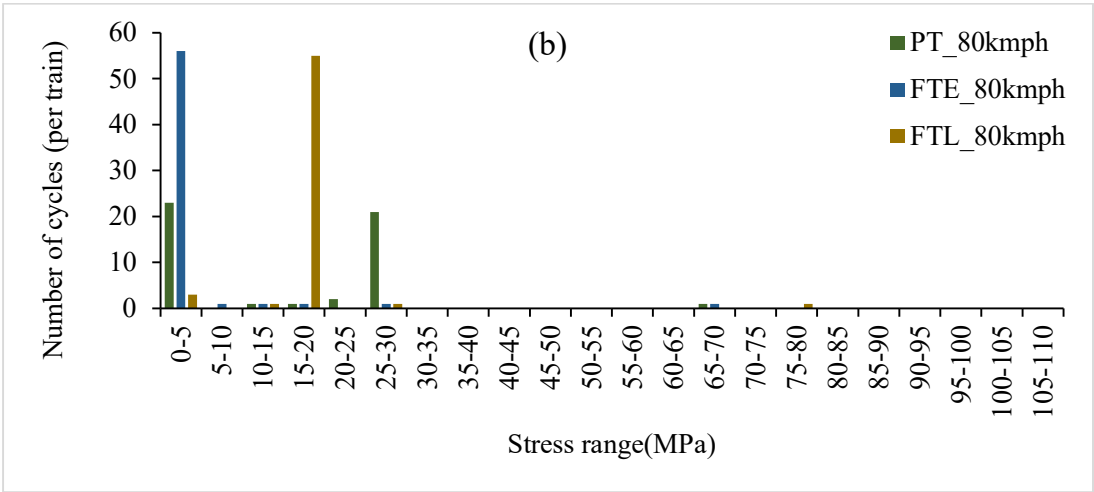

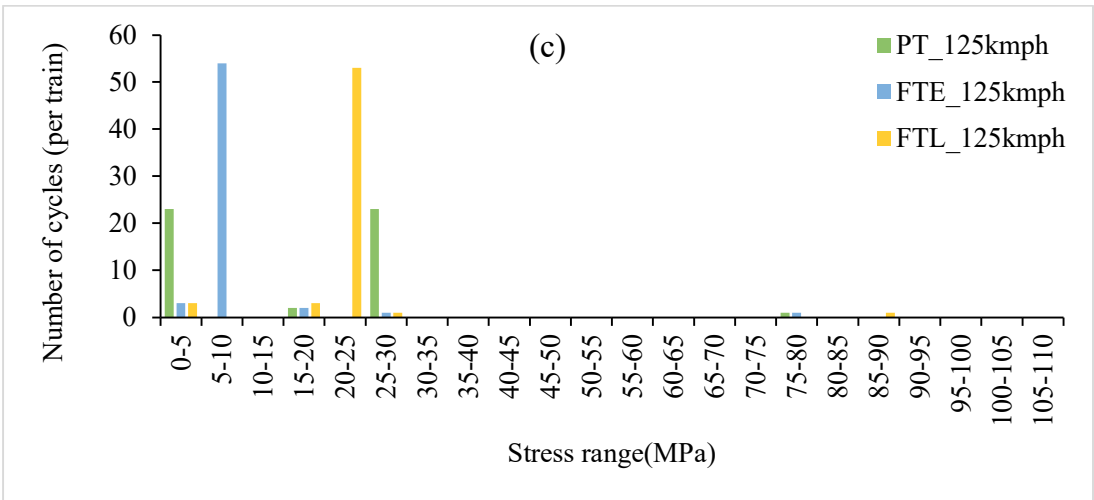

Figure 3.22: Stress histogram for member (cross beam-543 at mid) at stress band=5MPa. **(a)** PT, FTE & FTL at speed up to 50kmph **(b)** PT, FTE & FTL at speed equal to 80kmph **(c)** PT, FTE & FTL at speed equal to 125kmph

Remaining life of the bridge using stress life method is presented in Table 3.4.

Table 3.4: The remaining life of the bridge (Stress life method)

S. No.	Stress band	speed <50 kmph	speed =80 kmph	speed=125 kmph
1.	5 MPa	75.6 years	50.5 years	31.9 years
2.	10 MPa	64.3 years	64.3 years	35.1 years

3.4.2.2 Remaining life using LEFM approach

This method relates the growth of initial crack size to the number of repetitions, as can be seen from equation 3.3. Initial crack size is assumed and fracture toughness according to the material is obtained. The final crack length is calculated using equation 3.4, and on the basis of various material parameters, the initial and final crack lengths, remaining life of the bridge is calculated.

Using the LEFM approach remaining life of the bridge is assessed. In this approach, the initial crack length is assumed as 1.0mm. The maximum stress is determined for a given speed as the highest stress induced by the passage of a PT, FTE, or FTL train over the bridge. Similarly, for a given speed, the minimum stress is computed as the least stress caused by a PT, FTE, or FTL train passing over the bridge. Maximum stress due to traffic movement corresponding to speeds up to 50kmph, equal to 80kmph, and equal to 125 kmph is calculated 69.1 MPa, 77.24 MPa, and 86.96 MPa, respectively. Since the minimum stress for each speed case is small compressive value, it is taken as zero for all cases. Based on the initial crack length and considering room temperature and non-corrosive environment conditions and using material properties of mild steel, the final crack length is calculated

for each case (at speed< 50 kmph, speed=80 kmph & speed=125 kmph) and corresponding to each speed residual fatigue life has been estimated. Since the LEFM approach is depending the maximum and minimum stress induced due to the movement of rail traffic and not upon the stress range interval. The residual fatigue life of the existing bridge using this method is assessed separately.

Remaining life of the bridge using fracture mechanics approach is provided in Table 3.5.

Table 3.5: The remaining life of the bridge (Fracture mechanics approach)

S. No.	For speed <50 kmph	speed =80 kmph	speed=125 kmph
1.	91.6years	65.4years	45.7years

3.4.2.3 Comparison of life using stress-life method and LEFM approach

The lifespan of the bridge will also change if the stress range or stress band is altered. And the analysis has also looked at its impact. The residual life of the steel railway bridge assessed using both stress life method with stress bands of 5MPa,10MPa, and fracture approach can be seen in Figure 3.23. For the 5MPa stress band, at speeds up to 50 kmph, equal to 80 kmph, and equal to 125 kmph, the difference in remaining bridge life calculated using the stress life method and the LEFM approach is 16 years, 14.9 years, and 13.8 years, respectively. For the 10MPa stress band, at speeds up to 50 kmph, equal to 80 kmph, and equal to 125 kmph, the difference in remaining bridge life calculated using the stress life method and the LEFM approach is 27.3 years, 1.1 years, and 10.6 years, respectively.

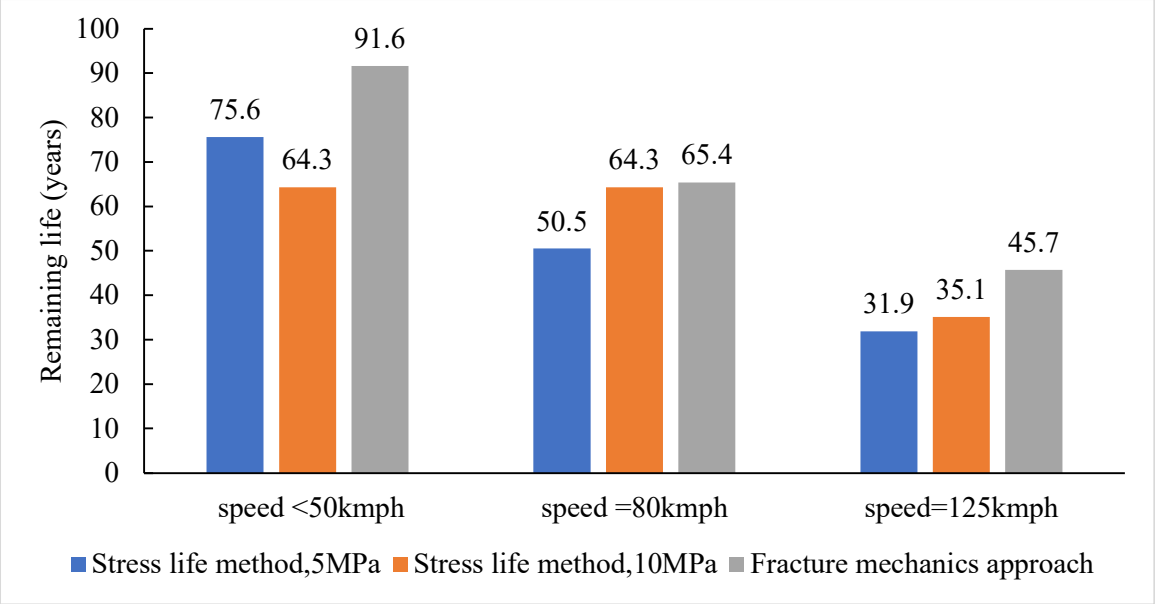

Figure 3.23: Comparison of the remaining life of the bridge using different methods

3.5 Concluding remarks

Following conclusions can be drawn from fatigue analysis of the steel truss bridge for rail loading “25T-2008” as per Railway Design and Standard Organization bridge rule (RDSO 2014).

1. Both the stress life method and the fracture mechanics approach show that the remaining life of the existing bridge decreases as speed increases at constant GMT.
2. After determining the residual life of the bridge using two separate stress bands, it can be concluded that a more precise figure can be derived as the stress band shrinks. As shown in Figure 3.23, at the 10MPa stress band, the bridge's lifespan is 64.3 years for trains running at speeds up to 50kmph or equal to 80kmph, which is not a reliable representation of its actual lifespan. However, if a stress band of 5MPa is utilized, the estimated lifespan of the bridge is 75.6 years and 50.5 years when the train runs at speeds up to 50 kmph and equal to 80 kmph, respectively.
3. It can also be deduced that when the stress band is smaller, the residual life does not necessarily increase or decrease in comparison to the residual life obtained with a larger stress band. When the stress range interval is 5 MPa, residual life is greater for speeds up to 50 kmph, and it is greater for speeds of 80 kmph and 125 kmph when the stress range interval is 10 MPa.
4. Residual life of the bridge obtained using fracture mechanics approach is on the conservative side in comparison to that obtained using the S-N curve-based approach.

5. The remaining life of the bridge as determined by the stress life at the stress band of 5MPa and LEFM approach has a maximum difference of 16 years, which is not a significant difference given the different assumptions made in each approach.
6. The difference in estimated remaining life between the LEFM approach and the stress life method at the 5 MPa stress band is almost uniform, but the same is exhibiting highly unpredictable behaviour at the 10 MPa stress band. Therefore, in the case of a lower stress band, a more precise and predictable remaining life can be obtained.
7. The proposed efficient and systematic approach can efficiently be used for the remaining life assessment of existing old steel railway bridges.